ACS Photonics

Letter

Cite This: ACS Photonics 2018, 5, 728−733

Selective Third-Harmonic Generation by Structured Light in Mie-Resonant Nanoparticles

Elizaveta V. Melik-Gaykazyan,*,† Sergey S. Kruk,‡ Rocio Camacho-Morales,‡ Lei Xu,‡ Mohsen Rahmani,‡ Khosro Zangeneh Kamali,‡ Aristeidis Lamprianidis,‡ Andrey E. Miroshnichenko,§ Andrey A. Fedyanin,† Dragomir N. Neshev,‡ and Yuri S. Kivshar‡

†Faculty of Physics, Lomonosov Moscow State University, Moscow 119991, Russia

‡Nonlinear Physics Centre, The Australian National University, Canberra ACT 2601, Australia

§School of Engineering and Information Technology, University of New South Wales, Canberra ACT 2600, Australia

Supporting Information

ABSTRACT: We study the third-harmonic generation by structured light in subwavelength silicon nanoparticles which support both electric and magnetic multipolar Mie resonances. By tailoring the vectorial structure of the pumping light, we may control both strength and polarization composition of the excited harmonic fields. In this way, we generate nonlinear fields with radial or azimuthal polarizations by addressing selectively a different type of multipolar Mie resonances, also enhancing or suppressing the optically induced nonlinear magnetic response.

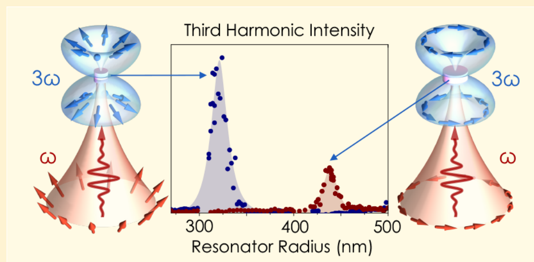

KEYWORDS: *nonlinear optics, third-harmonic generation, silicon nanoparticles, Mie resonances, vector beams, structured light*

Nonlinear nanophotonics is an active research field with a wide range of potential applications in the development of subwavelength nonlinear optical antennas, novel light sources, miniature lasers, and ultrafast nanoscale metadevices.[1] A strong confinement of the electromagnetic fields in resonant nanostructures can enhance substantially nonlinear optical effects, and it can be employed for the control of light at the nanoscale. To engineer specific nonlinear scattering from resonant nanoscale elements, the multipolar control of nonlinear response is required with interplay of several multipolar contributions of similar strength. This is hard to realize with plasmonic nanoparticles, but it becomes possible with dielectric and semiconductor nanoparticles[2−4] supporting Mie resonances.[5,6]

The study of nanoparticles made of high-refractive-index semiconductors (such as silicon, germanium, tellurium, AlGaAs, GaP) has emerged as a novel research direction in nanoscale photonics,[6] and it explores the multipolar and multimodal Mie resonances[7−9] for a range of meta-optics and metadevice applications with novel functionalities.[10,11] High-index nanoparticles support a variety of electric and magnetic dipolar and multipolar resonances that can be spectrally controlled and engineered independently,[12−14] and thus, all-dielectric resonant nanostructures offer unique opportunities for the study of nonlinear multipolar effects owing to low losses, in combination with magnetic response[15,16] and Fano resonances,[17,18] with the excitation of an anapole mode.[19,20] The interplay between different multipolar resonances determines directionality[21−23] and polarization structure[24,25] of both linear scattering and nonlinear light generation. This makes the control over selective multipolar excitations of high importance for nonlinear nanophotonics. While the multipolar nature of resonator modes is largely determined by geometry of a resonator and its constituent material, the efficiency of light coupling to a particular resonant mode strongly depends on the structure of the excitation beam.

Recently, Woźniak et al.[13] employed tightly focused light beams to address selectively different multipolar resonances of nanoparticles, exciting individual electric and magnetic multipoles even in the cases when they spectrally overlap. They also explored the effect of spatial degree of freedom that enables different coupling scenarios[26−28] within a single beam configuration with tunable and controllable directional emission.[29,30] Das et al.[14] suggested an analytical method for the study of the scattering of spherical nanoparticles by varying illumination properties, and in particular, they demonstrated the excitation of a quadrupole mode that cannot be accessed with conventional illumination. Tuning the unidirectional scattering from nanoantennas pumped by the combination of two radially and azimuthally polarized vector beams has been recently demonstrated by Xi et al.[31,32] It is highly desirable to apply this approach of selective excitation of different resonant modes to nonlinear nanophotonics and, thus, to generate selectively nonlinear harmonic fields with a full control of their spatial and polarization properties.

The idea to employ focused and structured vector beams for the second-harmonic generation (SHG) has been developed[33]

Received: October 28, 2017
Published: December 15, 2017

in recent years as a versatile tool to characterize nanowires compared to linear polarization.[34,35] A comprehensive review of microscopic techniques based on nonlinear optical processes in nanoscale structures and capabilities of nonlinear microscopy has been published recently by Bautista and Kauranen[36] who demonstrated that the vectorial focusing of conventional (linear and circular polarized) and unconventional (radial and azimuthal polarized) light can provide new capabilities for nonlinear microscopy.

In this Letter, we combine the recently developed concepts of high-index meta-optics and vector-field nonlinear microscopy and address an important question of the selective third-harmonic generation (THG) in subwavelength nanoparticles that support different types of Mie resonances. By tailoring the vectorial structure of the pumping light, we excite selectively different multipolar modes of the silicon nanodisks, thus, engineering the strength and polarization of the excited third-harmonic (TH) fields and enhancing or suppressing the optically induced nonlinear magnetic response. We believe our study will pave the way toward a novel type of nonlinear beam engineering via multipolar scattering properties of nanostructures and multipolar light−matter interactions at the nanoscale.

■ RESULTS AND DISCUSSIONS

In our study, we employ silicon nanodisks as high-index dielectric Mie resonators. We optimize the geometrical parameters of nanodisks where one nanodisk supports a strong electric quadrupole (EQ) Mie-type resonance at the wavelength of the optical pump (in our case, 1550 nm), and the other nanodisk supports a magnetic quadrupole (MQ) resonance at the pump wavelength. To couple efficiently to the quadrupole resonances and, thus, to efficiently generate TH, we use structured light.[37] Specifically, we employ a radially polarized vector beam to couple to the EQ resonator mode, and an azimuthally polarized beam for the MQ resonator mode (see Figure 1). We optimize geometrical parameters of nanodisks numerically by performing calculations of multipolar electromagnetic field decompositions of the scattering spectra.

Following the results of our calculations, we fabricate a set of 116 individual silicon nanodisks with radii ranging from 270 to 500 nm and a constant height of 700 nm on a glass substrate. The nanodisks are positioned far apart, with 10 μm distance between the neighbors, which makes them optically isolated. A concept image and scanning electron micrographs of silicon nanodisks are shown in Figure 2. The use of multiple sizes of resonant nanodisks and the fixed value of the pump wavelength of 1550 nm allows us to measure the dependence of the THG efficiency on multipolar spectrum while excluding the influence of material dispersion.

Figure 3a,b shows the difference in the multipolar structure of nanodisk scattering for two different cylindrical vector beams:[14,38] via radial (Figure 3a) and azimuthal (Figure 3b) polarizations. Specifically, a radially polarized pump beam excites the electric Mie resonances with the dominant contribution from the EQ accompanied by an electric dipole at around 310 nm disk radii and an anapole mode[39] for smaller disks (see details in the Supporting Information, section V). An azimuthal polarization, in turn, results in the excitation of magnetic multipoles dominated by the MQ resonance at around 460 nm disks radii.

To generate a TH signal, we tightly focus a femtosecond laser beam at 1550 nm wavelength onto each individual silicon nanodisk. Radial or azimuthal polarization of the laser beam is

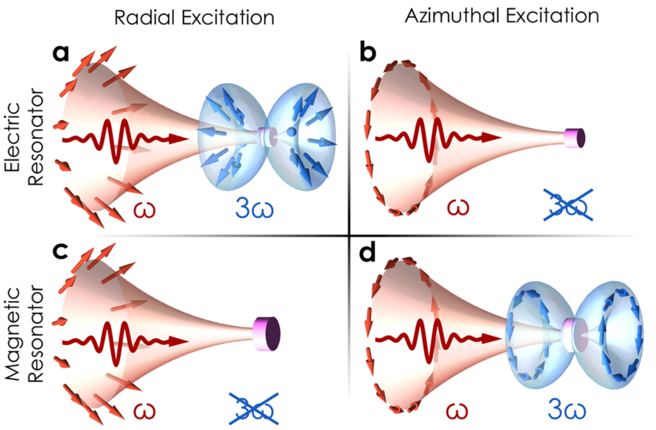

Figure 1. Third-harmonic generation in Si nanoparticles with structured light. (a) Electric quadrupole (EQ) Mie resonator efficiently generates electric third harmonic (TH) being pumped by a radially polarized beam. (b) Same EQ resonator does not generate TH being pumped by an azimuthally polarized beam. (c) Magnetic quadrupole (MQ) resonator does not generate TH being pumped by a radially polarized beam. (d) MQ resonator efficiently generates magnetic TH being pumped by an azimuthally polarized beam. Red and blue arrows visualize the electric field direction at the fundamental and TH frequencies, respectively.

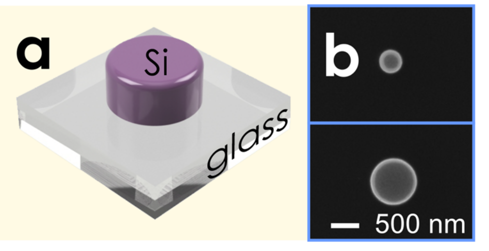

Figure 2. (a) Concept image of a sample: an individual silicon nanodisk on a glass substrate. (b) Scanning electron microscope images of two nanodisks with different radii.

mapped by the use of an all-dielectric metasurface reported previously.[40] Generated TH is collected by a confocal objective of 0.90 numerical aperture (NA) in the forward direction, and it is measured by a cooled CCD camera calibrated with a power meter (see details in Methods). Figure 3c,d shows experimentally measured and numerically calculated TH power in Si nanodisks for the two types of beams, respectively. The calculations are performed with a finite-element-method solver by COMSOL Multiphysics. Both the experiment and calculations demonstrate that the radially polarized pump enhances TH in the vicinity of the EQ resonance, and conversely, the azimuthally polarized pump enhances TH at the MQ resonance only. The TH profiles reveal high quality factors of the resonances. In the experiments, the TH signal produced by nonresonant nanodisks is 2 orders of magnitude smaller, and the TH signal from a substrate is negligible. The experimentally measured data are slightly shifted from numerically predicted resonance positions due to fabrication imperfections. We then numerically perform multipolar decomposition of the TH fields. This demonstrates that for the radially polarized pump the harmonic is dominated by the EQ response with smaller contributions from the electric dipole and higher-order electric multipoles. For the azimuthally polarized pump, the harmonic is dominated by MQ with a smaller contribution from a magnetic hexadecapole. Thus, radially polarized pump gen-

DOI: 10.1021/acsphotonics.7b01277
ACS Photonics 2018, 5, 728−733

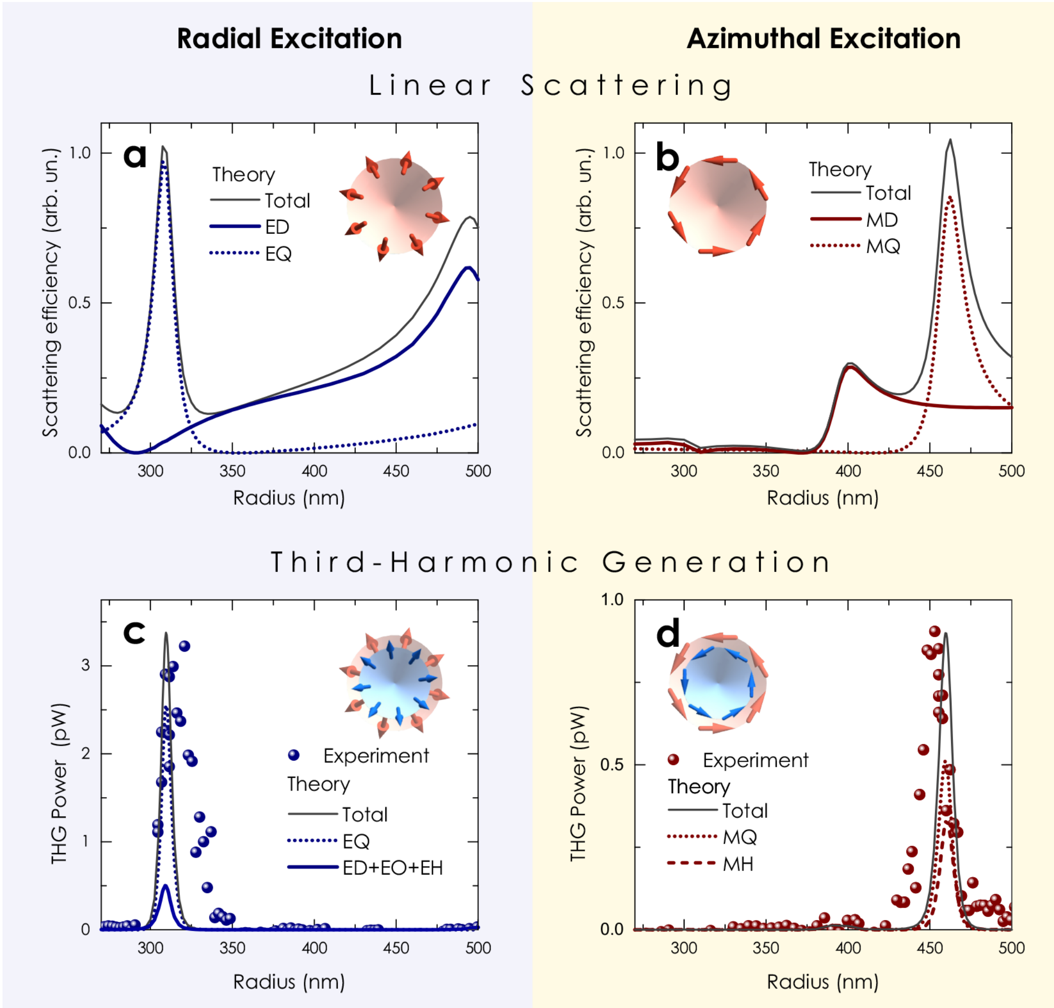

Figure 3. Selective third-harmonic generation (THG) with structured light. (a, b) Multipolar decomposition of linear light scattering by Si nanodisks with different radii for (a) radial and (b) azimuthal incident beams at the wavelength of 1550 nm. (c, d) Efficiency and multipolar structure of THG in Si nanodisks with different radii pumped at 1550 nm wavelength by (c) radial and (d) azimuthal beams, respectively. ED, an electric dipole; EO, an electric octupole; EH and MH, electric and magnetic hexadecapoles, respectively.

erates an electric third-harmonic signal in Si nanoresonators, and azimuthally polarized pump generates a magnetic third-harmonic signal in the nanoresonators.

We then focus on TH generated in two selected Si nanodisks being resonant for the radial and azimuthal pump, correspondingly. We investigate experimentally and numerically the radiation and polarization patterns of the TH fields. Figure 4a,b shows calculated three-dimensional radiation patterns for the two cases; and Figure 4c,d shows the planar projections of the radiation pattern onto the forward direction. Black arrows visualize the polarization structure of the TH fields. Experimentally retrieved radiation and polarization patterns of the TH fields are shown in Figure 4e,f, and they are in excellent agreement with our theory (see details in Methods). The radiation and polarization structure of the TH beams reveals experimentally either the electric or the magnetic origin of the harmonic fields for radial or azimuthal beams correspondingly.

In summary, we have observed the third-harmonic generation from silicon nanodisks excited at their electric and magnetic quadrupole Mie resonances. To efficiently couple the pump light to quadrupolar resonances, we have employed cylindrically polarized vector beams. We have observed selective enhancement and suppression of the excited harmonic fields, in dependence on the multipolar structure of the nanoscale resonators and the polarization structure of the pump beam. Our experimental findings are supported by the multipolar field decomposition and direct calculation of the nonlinear optical fields. These results demonstrate the capabilities of subwavelength dielectric nanoparticles to develop nonlinear beam engineering and actively tuned nanophotonic devices.

■ METHODS

Sample Fabrication. The silicon nanodisks shown in Figure 2 are fabricated on a glass substrate with 170 μm thickness. First, a 700 nm hydrogenerated amorphous silicon layer is deposited on the substrate by plasma-enhanced chemical vapor deposition (Oxford PlasmaLab System 100). Subsequently, a thin layer of a positive electro-resist is spin-coated on the sample, followed by the applied electron-beam lithography (Raith 150) and development. For this, a 50 nm Cr film is evaporated on the sample, followed by the lift-off process to generate Cr masks. By means of the reactive-ion etching processes, Cr disks are transferred to the silicon film. Finally, the residual Cr disks are removed via wet Cr etching. In order to avoid any organic layers on the top of the sample, the

DOI: 10.1021/acsphotonics.7b01277
ACS Photonics 2018, 5, 728−733

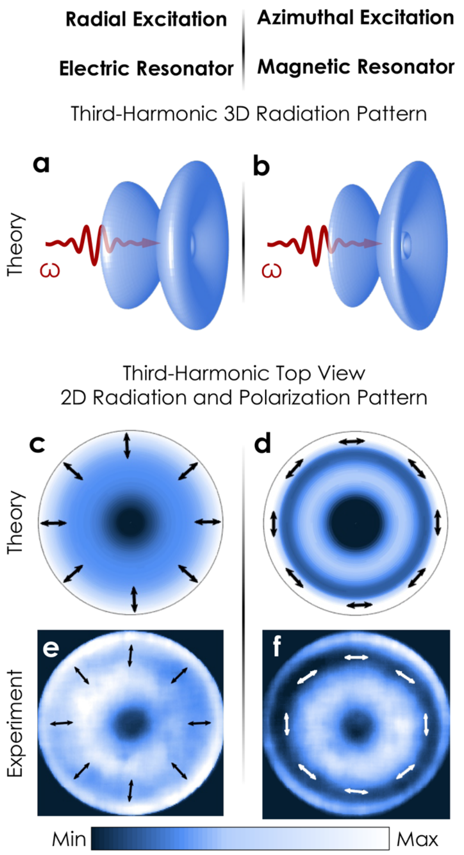

Figure 4. Directionality and polarization diagrams of TH signals from Si nanodisks pumped at (a, c, e) the EQ resonance by a radial beam, (b, d, f) the MQ resonance by an azimuthal beam. (a, b) Calculated 3D radiation patterns. (c, d) Calculated 2D projections of the TH radiation in the forward direction within numerical aperture (NA) 0.9. (e, f) Experimentally observed back-focal plane images of the TH radiation within NA 0.9. Arrows visualize the polarization of the TH field.

procedure of oxygen plasma cleaning is conducted, before an optical characterization.

Nonlinear Setup. For nonlinear optical measurements, we use a pulsed Er^{3+}-doped laser (PriTel, Inc. FFL-5 MHz, pulse duration of 600 fs, repetition rate of 5 MHz, fwhm of 3 nm) combined with an optical fiber amplifier (PriTel, Inc. HPFA-18) and operating at the wavelength of 1550 nm. A single disk is mounted on a three-dimensional stage, and it is placed at the normal incidence in a focal spot of two confocal air objective lenses Olympus LCPlan N (0.85 NA, 100× infrared), used for focusing the fundamental beam, and Olympus MPlanFL N (0.90 NA, 100× visible), used for collecting and collimating the transmitted TH radiation. The beam is focused from the front side of the sample. As a TH radiation detector, we use a cooled CCD camera (Starlight Xpress Ltd., SXVR-H9). The detected signal is filtered out by the colored (Thorlabs FESH0850) and dielectric (Thorlabs FGB18, FB520-10) glass set. The spectrum of a nonlinear signal is monitored with a spectrometer (Ocean Optics 6500), to verify the origin of the nonlinear signal. The TH power dependence is measured, and it is presented in the Supporting Information (section I). A pair of confocal lenses is used to build a back-focal plane image of the TH radiation onto a camera. The polarization structure of the back-focal plane images is analyzed with a quarter-wave plate and wire-grid polarizer mounted on motorized rotation stages. The method of the back-focal plane polarimetry is discussed previously.[41] To generate both radially and azimuthally polarized light from a linearly polarized laser beam, we use a *q*-plate metasurface fabricated by Kruk et al.[40] With the *q*-plate, we can flip the linear polarization of the laser beam from vertical to horizontal with the help of a half-wave plate and then obtain either radial or azimuthal polarizations, respectively. The spectrum of the pump beam is cleared up by a long-pass infrared filter (Thorlabs FEL 1000) before the first objective guarantees the excitation of an individual nanodisk.

Numerical Calculations. For numerical simulations of linear and nonlinear scattering, we use the finite-element-method solver in COMSOL Multiphysics in the frequency domain. All calculations are realized for a single nanodisk of a specific size. For the case of linear optical response, our calculation results show that the presence of a glass substrate did not lead to qualitative changes in multipolar decomposition spectra (the Supporting Information, section III). With this, we perform all nonlinear calculations for nanodisks in air, without a substrate. We employ the approach based on an undepleted pump approximation, using two steps to calculate the radiated nonlinear emission. First, we simulate the linear scattering at the fundamental wavelength, and then obtain the nonlinear polarization induced inside the nanodisk. Then, we employ it as a source for the electromagnetic simulation at the harmonic wavelength to obtain the generated TH field. A nonlinear susceptibility tensor $\chi^{(3)}$ is considered as a constant scalar value. The material dispersion data for amorphous silicon is taken as an experimental result of our ellipsometry measurements.

■ ASSOCIATED CONTENT

Ⓢ Supporting Information

The Supporting Information is available free of charge on the ACS Publications website at DOI: 10.1021/acsphotonics.7b01277.

Details of the optical characterization technique and schematic of the experimental setup (sections I and II), as well as numerical analysis (sections III–V) (PDF).

■ AUTHOR INFORMATION

Corresponding Author

*E-mail: melik@nanolab.phys.msu.ru.

ORCID

Elizaveta V. Melik-Gaykazyan: 0000-0001-7633-2376
Sergey S. Kruk: 0000-0003-0624-4033
Mohsen Rahmani: 0000-0001-9268-4793
Andrey E. Miroshnichenko: 0000-0001-9607-6621
Andrey A. Fedyanin: 0000-0003-4708-6895
Dragomir N. Neshev: 0000-0002-4508-8646
Yuri S. Kivshar: 0000-0002-3410-812X

Notes

The authors declare no competing financial interest.

■ ACKNOWLEDGMENTS

The authors thank Jon Schuller, Peter Banzer, Natalia Litchinitser, and Martti Kauranen for fruitful discussions and suggestions. E.M.G. acknowledges the funding from the Student Mobility Scholarship of the President of the Russian Federation. R.C.M. acknowledges a grant from Consejo Nacional de Ciencia y Tecnología (CONACYT), México. The authors acknowledge a support of the Australian Research

Council (ARC) and the Russian Ministry of Education and Science (#14.W03.31.0008).

■ REFERENCES

(1) Kauranen, M.; Zayats, A. V. Nonlinear plasmonics. *Nat. Photonics* **2012**, *6*, 737–748.

(2) Sanatinia, R.; Swillo, M.; Anand, S. Surface second-harmonic generation from vertical GaP nanopillars. *Nano Lett.* **2012**, *12*, 820–826.

(3) Sanatinia, R.; Anand, S.; Swillo, M. Modal engineering of second-harmonic generation in single GaP nanopillars. *Nano Lett.* **2014**, *14*, 5376–5381.

(4) Cambiasso, J.; Grinblat, G.; Li, Y.; Rakovich, A.; Cortés, E.; Maier, S. A. Bridging the gap between dielectric nanophotonics and the visible regime with effectively lossless gallium phosphide antennas. *Nano Lett.* **2017**, *17*, 1219–1225.

(5) Smirnova, D.; Kivshar, Y. S. Multipolar nonlinear nanophotonics. *Optica* **2016**, *3*, 1241–1255.

(6) Kuznetsov, A. I.; Miroshnichenko, A. E.; Brongersma, M. L.; Kivshar, Y. S.; Luk'yanchuk, B. Optically resonant dielectric nanostructures. *Science* **2016**, *354*, aag2472.

(7) Mie, G. Beiträge zur Optik trüber Medien, speziell kolloidaler Metalllösungen. *Ann. Phys. (Berlin, Ger.)* **1908**, *25*, 377–445.

(8) Kuznetsov, A. I.; Miroshnichenko, A. E.; Fu, Y. H.; Zhang, J.; Luk'yanchuk, B. Magnetic light. *Sci. Rep.* **2012**, *2*, 492.

(9) Evlyukhin, A. B.; Novikov, S. M.; Zywietz, U.; Eriksen, R. L.; Reinhardt, C.; Bozhevolnyi, S. I.; Chichkov, B. N. Demonstration of magnetic dipole resonances of dielectric nanospheres in the visible region. *Nano Lett.* **2012**, *12*, 3749–3755.

(10) Kivshar, Y. S.; Miroshnichenko, A. E. Meta-optics with Mie resonances. *Opt. Photonics News* **2017**, *28*, 24–31.

(11) Kruk, S.; Kivshar, Y. Functional meta-optics and nanophotonics govern by Mie resonances. *ACS Photonics* **2017**, *4*, 2638–2649.

(12) Staude, I.; Miroshnichenko, A. E.; Decker, M.; Fofang, N. T.; Liu, S.; Gonzales, E.; Dominguez, J.; Luk, T. S.; Neshev, D. N.; Brener, I.; Kivshar, Y. Tailoring directional scattering through magnetic and electric resonances in subwavelength silicon nanodisks. *ACS Nano* **2013**, *7*, 7824–7832.

(13) Woźniak, P.; Banzer, P.; Leuchs, G. Selective switching of individual multipole resonances in single dielectric nanoparticles. *Laser Photon. Rev.* **2015**, *9*, 231–240.

(14) Das, T.; Iyer, P. P.; DeCrescent, R. A.; Schuller, J. A. Beam engineering for selective and enhanced coupling to multipolar resonances. *Phys. Rev. B: Condens. Matter Mater. Phys.* **2015**, *92*, 241110.

(15) Shcherbakov, M. R.; Neshev, D. N.; Hopkins, B.; Shorokhov, A. S.; Staude, I.; Melik-Gaykazyan, E. V.; Decker, M.; Ezhov, A. A.; Miroshnichenko, A. E.; Brener, I.; Fedyanin, A. A.; Kivshar, Y. S. Enhanced third-harmonic generation in silicon nanoparticles driven by magnetic response. *Nano Lett.* **2014**, *14*, 6488–6492.

(16) Melik-Gaykazyan, E. V.; Shcherbakov, M. R.; Shorokhov, A. S.; Staude, I.; Brener, I.; Neshev, D. N.; Kivshar, Y. S.; Fedyanin, A. A. Third-harmonic generation from Mie-type resonances of isolated all-dielectric nanoparticles. *Philos. Trans. R. Soc., A* **2017**, *375*, 20160281.

(17) Shorokhov, A. S.; Melik-Gaykazyan, E. V.; Smirnova, D. A.; Hopkins, B.; Chong, K. E.; Choi, D.-Y.; Shcherbakov, M. R.; Miroshnichenko, A. E.; Neshev, D. N.; Fedyanin, A. A.; Kivshar, Y. S. Multifold enhancement of third-harmonic generation in dielectric nanoparticles driven by magnetic Fano resonances. *Nano Lett.* **2016**, *16*, 4857–4861.

(18) Limonov, M. F.; Rybin, M. V.; Poddubny, A. N.; Kivshar, Y. S. Fano resonances in photonics. *Nat. Photonics* **2017**, *11*, 543–554.

(19) Grinblat, G.; Li, Y.; Nielsen, M. P.; Oulton, R. F.; Maier, S. A. Enhanced third harmonic generation in single germanium nanodisks excited at the anapole mode. *Nano Lett.* **2016**, *16*, 4635–4640.

(20) Grinblat, G.; Li, Y.; Nielsen, M. P.; Oulton, R. F.; Maier, S. A. Efficient third harmonic generation and nonlinear subwavelength imaging at a higher-order anapole mode in a single germanium nanodisk. *ACS Nano* **2017**, *11*, 953–960.

(21) Person, S.; Jain, M.; Lapin, Z.; Sáenz, J. J.; Wicks, G.; Novotny, L. Demonstration of zero optical backscattering from single nanoparticles. *Nano Lett.* **2013**, *13*, 1806–1809.

(22) Carletti, L.; Locatelli, A.; Neshev, D.; de Angelis, C. Shaping the radiation pattern of second-harmonic generation from AlGaAs dielectric nanoantennas. *ACS Photonics* **2016**, *3*, 1500–1507.

(23) Wang, L.; Kruk, S. S.; Xu, L.; Rahmani, M.; Smirnova, D.; Solntsev, A.; Kravchenko, I.; Neshev, D. N.; Kivshar, Y. S. Shaping the third-harmonic radiation from silicon nanodimers. *Nanoscale* **2017**, *9*, 2201–2206.

(24) Camacho-Morales, R.; Rahmani, M.; Kruk, S. S.; Wang, L.; Xu, L.; Smirnova, D. A.; Solntsev, A. S.; Miroshnichenko, A.; Tan, H. H.; Karouta, F.; Naureen, Sh.; Vora, K.; Carletti, L.; de Angelis, C.; Jagadish, Ch.; Kivshar, Y. S.; Neshev, D. N. Nonlinear generation of vector beams from AlGaAs nanoantennas. *Nano Lett.* **2016**, *16*, 7191–7197.

(25) Kruk, S. S.; Camacho-Morales, R.; Xu, L.; Rahmani, M.; Smirnova, D.; Wang, L.; Tan, H. H.; Jagadish, C.; Neshev, D. N.; Kivshar, Y. S. Nonlinear optical magnetism revealed by second-harmonic generation in nanoantennas. *Nano Lett.* **2017**, *17*, 3914–3918.

(26) Müller, J.; Banzer, P.; Quabis, S.; Peschel, U.; Leuchs, G. Waveguide properties of single subwavelength holes demonstrated with radially and azimuthally polarized light. *Appl. Phys. B: Lasers Opt.* **2007**, *89*, 517–520.

(27) Banzer, P.; Kindler, J.; Quabis, S.; Peschel, U.; Leuchs, G. Extraordinary transmission through a single coaxial aperture in a thin metal film. *Opt. Express* **2010**, *18*, 10896–10904.

(28) Banzer, P.; Peschel, U.; Quabis, S.; Leuchs, G. On the experimental investigation of the electric and magnetic response of a single nano-structure. *Opt. Express* **2010**, *18*, 10905–10923.

(29) Neugebauer, M.; Woźniak, P.; Bag, A.; Leuchs, G.; Banzer, P. Polarization controlled directional scattering for nanoscopic position sensing. *Nat. Commun.* **2016**, *7*, 11286.

(30) Neugebauer, M.; Bauer, T.; Banzer, P.; Leuchs, G. Polarization tailored light driven directional optical nanobeacon. *Nano Lett.* **2014**, *14*, 2546–2551.

(31) Xi, Z.; Wei, L.; Adam, A. J. L.; Urbach, H. P. Broadband active tuning of unidirectional scattering from nanoantenna using combined radially and azimuthally polarized beams. *Opt. Lett.* **2016**, *41*, 33–36.

(32) Wei, L.; Bhattacharya, N.; Urbach, H. P. Adding a spin to Kerker's condition: angular tuning of directional scattering with designed excitation. *Opt. Lett.* **2017**, *42*, 1776–1779.

(33) Bautista, G.; Huttunen, M. J.; Mäkitalo, J.; Konito, J. M.; Simonen, J.; Kauranen, M. Second-harmonic generation imaging of metal nano-objects with cylindrical vector beams. *Nano Lett.* **2012**, *12*, 3207–3212.

(34) Bautista, G.; Mäkitalo, J.; Chen, Y.; Dhaka, V.; Grasso, M.; Karvonen, L.; Jiang, H.; Huttunen, M. J.; Huhtio, T.; Lipsanen, H.; Kauranen, M. Second-harmonic generation imaging of semiconductors nanowires with focused vector beams. *Nano Lett.* **2015**, *15*, 1564–1569.

(35) Turquet, L.; Kakko, J. P.; Zang, X.; Naskali, L.; Karvonen, L.; Jiang, H.; Huhtio, T.; Kauppinen, E.; Lipsanen, H.; Kauranen, M.; Bautista, G. Tailorable second-harmonic generation from an individual nanowire using spatially phase-shaped beams. *Laser Photon. Rev.* **2017**, *11*, 1600175.

(36) Bautista, G.; Kauranen, M. Vector-field nonlinear microscopy of nanostructures. *ACS Photonics* **2016**, *3*, 1351–1370.

(37) Litchinitser, N. M. Structured light meets structured matter. *Science* **2012**, *337*, 1054–1055.

(38) Das, T.; Schuller, J. A. Dark modes and field enhancements in dielectric dimers illuminated by cylindrical vector beams. *Phys. Rev. B: Condens. Matter Mater. Phys.* **2017**, *95*, 201111.

(39) Miroshnichenko, A. E.; Evlyukhin, A. B.; Yu, Y. F.; Bakker, R. M.; Chipouline, A.; Kuznetsov, A. I.; Luk'yanchuk, B.; Chichkov, B. N.; Kivshar, Y. S. Nonradiating anapole modes in dielectric nanoparticles. *Nat. Commun.* **2015**, *6*, 8069.

DOI: 10.1021/acsphotonics.7b01277
ACS Photonics 2018, 5, 728–733

(40) Kruk, S.; Hopkins, B.; Kravchenko, I. I.; Miroshnichenko, A.; Neshev, D. N.; Kivshar, Y. S. Broadband highly efficient dielectric metadevices for polarization control. *APL Photonics* **2016**, *1*, 030801.
(41) Kruk, S. S.; Decker, M.; Staude, I.; Schlecht, S.; Greppmair, M.; Neshev, D. N.; Kivshar, Y. S. Spin-polarized photon emission by resonant multipolar nanoantennas. *ACS Photonics* **2014**, *1*, 1218–1223.

DOI: 10.1021/acsphotonics.7b01277
ACS Photonics 2018, 5, 728–733